hibit large photovoltage in visible light where absorption in the oxide film is negligible, and further that the photovoltage is independent of the thickness of the oxide film, are convincing evidence against the hypothesis of a bulk effect in the oxide. Detailed studies have been made[6–8] of photo effects on both anodic and thermally grown thin oxide films sandwiched between the parent metal film and a thin metal film counterelectrode and definite evidence[7] has been found for the origin of photoelectrons at the two metal-oxide interfaces. The metal-oxide interfaces behave like graded gap semiconductors[6] due to the graded composition of the film. The gradation determines the photoconductivity and photovoltage of the structure. Thermal oxidation yields a less steep gradation as compared with anodic oxidation, and hence a larger photocurrent and photovoltage are obtained in thermally oxidized films.

The electrode materials do not contribute directly to the photo electrons. The polarity and the magnitude of photovoltage, however, depends on the intrinsic fields[8] in the insulator which are controlled by the space-charge and the work functions of the electrode materials. This demonstrates the significance of a suitable choice of electrode materials. The stronger the rectification, the higher the photovoltage obtained. With slightly asymmetric structures[7] of type Nb-Nb oxide-Al or Al-Al oxide-Al, a reversal of photovoltage with time and direction of illumination is observed and is explained by the fact that photoelectrons originate at both interfaces.

The sputtered niobium films (~5000 Å) are oxidized at about 400°C in an atmosphere of oxygen for about one half hour. Thin film counterelectrodes are deposited by evaporation of a suitable metal. The typical structures are squares of dimensions $\frac{1}{16}$ in × $\frac{1}{16}$ in. Photocurrent and photovoltage as a function of the intensity of light incident on Nb-Nb oxide-Au sandwich are shown in Fig. 1. These curves have been obtained with the light of wavelength $\lambda = 5450$ Å. Similar curves are obtained with light from a tungsten filament source. As mentioned above, the maximum value of photocurrent and photovoltage depends very strongly on the method of preparation of the oxide film as well as on the counterelectrode film. Photovoltages and photocurrent density as high as 0.8 v and 5 μa/cm^2 can be obtained.

The linear relation between the photocurrent and light intensity is noteworthy. The photovoltage is approximately given as[2]

$$V_{\text{photo}} \propto V_m(1 - e^{-Kt})$$

where

V_m = the maximum photovoltage,

t = time and K is a constant proportional to the intensity of light.

The similarity of the V_{photo} vs L curve with that of the selenium barrier-layer photocell is interesting. The time dependence of photovoltage for different levels of illumination is shown in Fig. 2. The slow response time is typical of trap filled photoconductors.

The variation of photocurrent with photovoltage for different intensities of light is shown in Fig. 3. The photocell behaves as a constant current generator for low intensities and is analogous to a p-n junction photocell. The observed behavior is due to high internal impedance at low intensity levels. At higher intensities, regions of both constant current and constant voltage are observed. The observation of nonlinear characteristics contradicts the postulate of a p-n or p-i-n type structure for the oxide film. It is significant that for anodized films of Ta[3] and Ti[5] a linear relationship between the photocurrent and photovoltage has been reported. Such a linear relationship is not useful for practical purposes as a photocell.

The thin film niobium oxide photocell offers the advantages of microminiaturization and should also be less susceptible to the radiation damage as compared with the p-n junction photocells. The efficiency of conversion is, however, poor and is about 100 times smaller than that of the commonly used semiconducting silicon photocells. Although the spectral response of such cells has not been studied in detail as yet, no selective response in the visible region has been found.

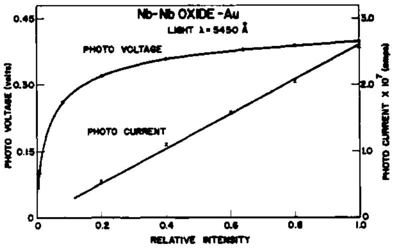

Fig. 1—The dependence of photovoltage and photocurrent on the intensity of light ($\lambda = 5500$ Å).

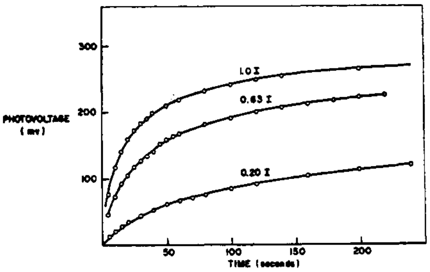

Fig. 2—The variation of photovoltage with time for different intensities of illumination (using tungsten filament light).

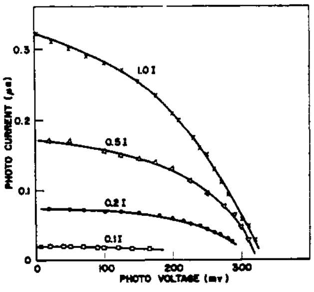

Fig. 3—The relation between photocurrent and photovoltage (using tungsten filament light).

K. L. Chopra
L. C. Bobb
Philco Scientific Lab.
Blue Bell, Pa.

---

[6] K. L. Chopra and L. C. Bobb, "Semiconducting properties of Nb oxide films," *J. Electrochem. Soc.*, vol. 110, p. 168C; August, 1963.

[7] K. L. Chopra, "Origin of photoelectrons in thin film metal-oxide-metal structures," to be published in *Appl. Phys. Letters*.

[8] K. L. Chopra and L. C. Bobb, "Photoeffects in thin oxide film sandwich structures," to be published in *J. Appl. Phys.*

Population Inversion Between Bound and Repulsive Molecular Electronic States by Two-Temperature Equilibrium*

This correspondence proposes a new class of gas laser systems, well suited for high-power operation, in which the upper energy level of the laser transition is predominately populated by direct electron impact at the electron temperature, and the lower energy level of the laser transition is controlled by collisions between gas atoms at the heavy particle temperature. An example of such a system for direct two-temperature operation is a molecule that has an upper bound electronic state and a lower repulsive electronic state, for example the bound $a^3\Sigma_g^+$ and the repulsive $b^3\Sigma_u^+$ states of hydrogen, which are shown in Fig. 1. The criterion for inversion is that the electron temperature be made sufficiently greater than the gas temperature, a condition found in high current density arcs running under steady-state conditions at moderate pressure.

For the case of hydrogen, radiation from a to the ground state is not allowed. The a-to-b transition is the only allowed radiative transition from the a state.[1,2] Population inversion between a and b is achieved because of the very short lifetime of the b state which dissociates spontaneously. The lifetime of the b state can be approximately calculated from the acceleration the hydrogen atoms received from the repulsive potential. This time can be expressed as $\tau(b) = (2MV_b)^{1/2}(dV/dr)^{-1}$, where V_b is the energy measured up from the dissociation limit of the X state and dV/dr is evaluated at V_b. For example, at the internuclear separation corresponding to the minimum of the a state, $\tau(b)$ has the value 10^{-14} sec.

A simple two-temperature calculation has been made in order to estimate the inversion which could be achieved in the hydrogen system under certain circumstances. In this model, the following proc-

---

* Received October 16, 1963. This work has been supported by Headquarters, Ballistic Systems Division, Air Force Systems Command, United States Air Force, under Contract AF 04(694)-33.

[1] G. Herzberg, "Molecular Spectra and Molecular Structure," D. Van Nostrand, Co., Inc., New York, N. Y., p. 403; 1950.

[2] H. M. James and A. S. Coolidge, "Continuous spectra of H_a and D_a," *Phys. Rev.*, vol. 55, pp. 184–190; January, 1939.

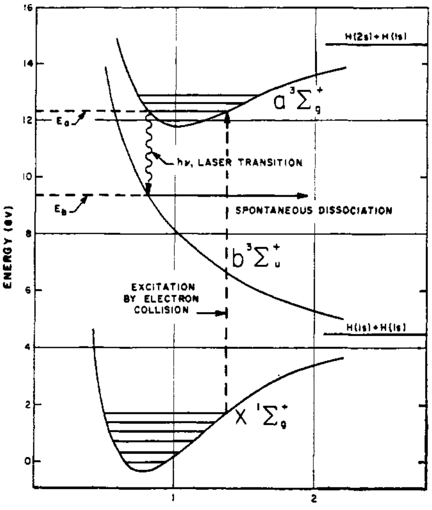

Fig. 1—The potential energy diagram for molecular hydrogen showing the ground state *X* and the *a* and *b* triplet electronic states which give rise to the continuous spectrum of hydrogen long used as a light source in UV absorption spectroscopy. The radiative lifetime of the *a* state has been theoretically calculated as 10^{-8} sec.[2] The *b* state spontaneously dissociates in about 10^{-14} sec. It is, therefore, possible to invert the *a* and *b* populations even when collision times with electrons become much shorter than the radiative lifetime of the upper state. A typical excitation, radiation, and dissociation path is shown.

esses are assumed in equilibrium:

$$H_2(a^3\Sigma_g) \overset{T_e}{\rightleftharpoons} H_2(X^1\Sigma_g)$$

$$H_2(b^3\Sigma_u) \overset{T}{\rightleftharpoons} 2H(1s)$$

$$H_2(X^1\Sigma_g) \overset{T}{\rightleftharpoons} 2H(1s)$$

where T_e is the electron temperature and T is the gas temperature. If these equilibria are satisfied, the ratio of *a* to *b* state populations is given as $[H_2(a)]/[H_2(b)] = \exp(E_b/T - E_a/T_e)$. $[H_2(b)]$ is defined as the average concentration of molecules in the repulsive state at the same internuclear separation as the $a^3\Sigma_g$ for a particular frequency of radiation. The criterion for inversion is then that $T_e/T > E_a/E_b = 1.50$ for the $v=0$ level, and $E_a/E_b = 1.34$ and 1.27 for the small internuclear separation side of the *a* state potential curve for the $v=1$ and $v=2$ levels, respectively. Fig. 2 is a plot of $[H_2(a)]/[H_2(b)]$ vs T_e/T at various values of T_e for the $v=0$ level of the *a* state, and indicates that enormous inversions are possible for relatively modest values of T_e/T.

The radiation from this *a*-to-*b* transition appears as a broad continuum extending from 1800 Å to 5000 Å. Assuming a large inversion ratio, the fractional gain per unit length $\Delta I/I\Delta x$ can be expressed[3] as $\Delta I/I\Delta x = \lambda^5 P(\lambda)/4\pi\hbar c^2$ where $P(\lambda)$ is the spontaneous radiation power per unit volume, wavelength, and solid angle. In preliminary arc experiments at 5 mm Hg pressure of H_2 and 500 amp/cm², we have observed $P(\lambda = 3500$ Å$) = 40$ watts/cm³-μ-ster, which would correspond to a gain of about 0.2 per cent per meter. We also estimate theoretically from the rate equations and from radiation measurements that under the conditions of the experiment $T_e = 3$ ev and $T_e/T = 7$. This implies the large inversion ratio of 9×10^4, limited by direct electron excitation from *X* to *b*. We expect practical gains of a few percent to be achievable at higher pressure and current density, at the expense of less population inversion. The threshold power for laser oscillation of a system of this kind is at a power level in the kilowatt range. Correspondingly, very high saturation power should also be possible.

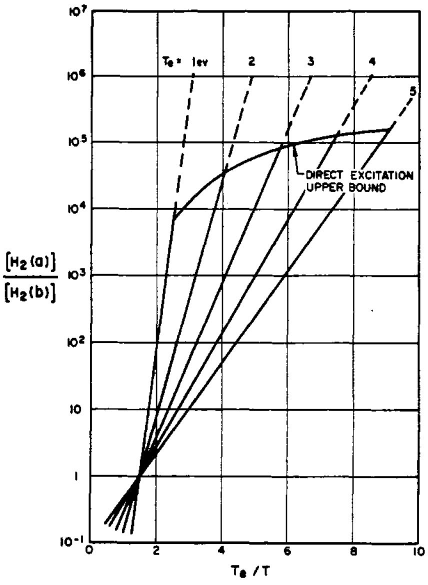

Fig. 2—The population inversion ratio between the *a* and *b* states as a function of the ratio of the electron temperature to the gas temperature at various electron temperatures. The curved line is an estimate from published cross sections[4] of the upper bound to the inversion ratio because of direct excitation from *X* to *b* by electron impact.

Many other bound-repulsive molecular systems exist,[1] such as He_2, Ne_2, Ar_2, Kr_2, Xe_2, Hg_2 and Cd_2. The first five radiate in the vacuum UV and all seven have repulsive ground states, unlike hydrogen. Many molecules may also have favorable bound-repulsive state pairs, for which the repulsive state does not dissociate into two ground state atoms. Hydrogen was chosen for our preliminary investigation because its properties are better known and it is experimentally easiest to handle.

As this correspondence was being prepared for publication, it was pointed out to the authors that the basic theoretical idea had appeared in an article by Houtermans in 1960.[5]

D. A. Leonard
J. C. Keck
Avco-Everett Research Lab.
Everett, Mass.
M. M. Litvak
M.I.T. Lincoln Lab.
Lexington, Mass.
Formerly with Avco-Everett
Research Lab.

---

[3] A. C. G. Mitchell and M. W. Zemansky, "Resonance Radiation and Excited Atoms" Cambridge University Press, Cambridge, England, p. 92; 1961.

[4] H. S. W. Massey and E. H. S. Burhop, "Electronic and Ionic Impact Phenomena," Clarendon Press, Oxford, England, p. 237; 1952.

[5] F. G. Houtermans, "Über Maser-Wirkung im optischen Spektralgebiet und die Möglichkeit absolut negativer Absorption für einige Fälle von Molekülspektren (Licht-Lawine)," *Helv. Phys. Acta*, vol. 33, p. 933; November, 1960.

A Consideration of Two Ensemble Methods for Treating a Certain Class of Stochastic Problems*

In a recent U.C.L.A. Engineering Seminar Paper, this author derived some results concerning the second-moment description of the responses of linear stochastic systems to stochastic inputs. The specific second moment used was the nonstationary autocorrelation function of the form $R(t_1, t_2)$.

The type of linear system considered was the following:

$$\{z(L)\}\{y(t)\} = \{x(t)\}, \qquad a \leq t \leq b$$

where $\{z(L)\}$ is a linear stochastic integro-differential operator of the form

$$\{z(L)\} \overset{\Delta}{=} \sum_{n=-N_1}^{N_2} \alpha_n L^n; N_1, N_2 \geq 0, \alpha_n = \text{constant}$$

$$Lf(t) \overset{\Delta}{=} \sum_{i=0}^{J} \{v_i(t)\} f^{(i)}(t).$$

$\{x(t)\}$ is the stochastic input to the linear system, $\{y(t)\}$ the stochastic response and the $\{v_i(t)\}$ arise from the stochastic variation of the system.

Two methods of solution were considered:

1) *Transform-Ensemble Method*

Define: the following autocorrelation functions.

$$R_y(t_1, t_2) \overset{\Delta}{=} E_y\{y(t_1)y(t_2)\}$$
$$R_x(t_1, t_2) \overset{\Delta}{=} E_x\{x(t_1)x(t_2)\}$$
$$\hat{R}_M(\lambda_1, \lambda_2) \overset{\Delta}{=} E_M\{M(\lambda_1)M(\lambda_2)\},$$

where $E_y\{\cdot\}$ is the expected value of the process $\{\cdot\}$ with respect to the appropriate probability law of *y*. $\{M(\lambda)\}$ is an ensemble of algebraic functions resulting from transforming the ensemble of operators $\{z(L)\}$. The variables t_1 and t_2 are real variables and λ_1 and λ_2 are complex variables. Define

$$\hat{R}_X(\lambda_1, \lambda_2) \overset{\Delta}{=} T_{t_1}T_{t_2}R_x(t_1, t_2),$$

where $T_{t_1}T_{t_2}$ represents an iterated direct integral transformation. The following result was obtained:

$$R_y(t_1, t_2) = T_{\lambda_1}{}^{-1}T_{\lambda_2}{}^{-1}\hat{R}_M(\lambda_1, \lambda_2)\hat{R}_X(\lambda_1, \lambda_2),$$

where $T_{\lambda_1}{}^{-1}T_{\lambda^2}{}^{-1}$ represents an iterated inverse transformation.

2) *Green's Function-Ensemble Method*

Given

$$\{z(L)\}\{y(t)\} = \{x(t)\}, \qquad a \leq t \leq b,$$

as before, formally define an ensemble of Green's functions as

$$\{z(L)\}\{g(t; t')\} \overset{\Delta}{=} \delta(t - t').$$

The following result was obtained:

$$R_y(t_1, t_2) = \int_a^b dt_1' \int_a^b dt_2' R_g(t_1, t_2; t_1', t_2') R_x(t_1', t_2'),$$

---

* Received June 6, 1963.